Journal of Low Temperature Physics, Vol. 29, Nos. 3/4, 1977

Solving the Eliashberg Equations by Means of *N*-Point Padé Approximants

H. J. Vidberg and J. W. Serene*,†

Department of Technical Physics and Low Temperature Laboratory, Helsinki University of Technology, Espoo, Finland

(Received April 26, 1977)

We study the use of N*-point Padé approximants to analytically continue the complex frequency Green's function from the Matsubara points to the real frequency axis. The method is applied to solutions of the Eliashberg equations and the approximants are compared with tabulated real frequency results. The overall agreement is good. We further show that the method can serve to make imaginary frequency calculations consistent with real frequency calculations by fixing the pseudopotential* μ^* *to the energy gap* Δ_0.

1. INTRODUCTION

At nonzero temperatures the calculation of the Green's function of a strong coupling superconductor is usually performed in two steps: First the diagrammatic analysis is carried out for the thermodynamic Green's function defined at the discrete imaginary (Matsubara) frequencies

$$i\omega_n = i\pi T(2n-1) \qquad \text{(fermions)} \tag{1}$$

The Fourier transform of the retarded real-time Green's function is then obtained by an analytic continuation in the upper half complex frequency plane to the real frequency axis. In general this continuation is made without explicitly calculating the Green's function at the Matsubara points. Unfortunately, the analytically continued equations for the real frequency Green's function are more complicated than the original equations, because the frequency dependence in the continued equations is determined by singular integral equations, while the original equations contain only discrete frequency sums.

*Permanent address: Department of Physics, State University of New York at Stony Brook, Stony Brook, New York.

†Nordic Institute for Theoretical Atomic Physics (NORDITA) Fellow 1975–76 at Research Institute for Theoretical Physics, University of Helsinki, Finland.

In this work we propose a different procedure: We first calculate the Green's function at the Matsubara points and then continue to real frequencies by fitting a rational fraction to the calculated values. If we use N Matsubara points, the corresponding rational approximation is an N-point Padé approximant. This type of approximation is the simplest that can simulate the nonanalyticities of the Green's function in the lower half complex frequency plane, which in turn determine the shape of the function on the real axis. Another advantage is that the correct asymptotic behavior can be directly incorporated in the representation by fixing the difference of the orders of the polynomials in the numerator and denominator.

Section 2 summarizes the outcomes of numerous tests we performed to study the resolution that could be obtained with the Padé method and to optimize the choice of input points. In the first part of Section 3 we apply the method to solutions of the imaginary frequency Eliashberg equations in the theory of strong coupling superconductivity, and compare the results with tabulated solutions of the real frequency equations. We find good overall agreement. The moderate computer time needed makes this way of solving the Eliashberg equations very attractive. Finally, we discuss the problem of choosing the Coulomb pseudopotential for imaginary frequency calculations of thermodynamic properties. We use Padé approximants to adjust the pseudopotential so that the calculated energy gap agrees with the experimental value. We then use this pseudopotential to calculate the transition temperature T_c. The T_c's calculated in this way generally agree better with measured T_c's than do the T_c's calculated from the pseudopotential used to extract the real-frequency phonon function $\alpha^2 F$.

2. RESOLUTION AND CHOICE OF INPUT POINTS

A fast algorithm for calculating an N-point Padé approximant from the values of a function at N complex points z_i $(i = 1, \ldots, N)$ is described in the appendix. This recursive procedure gives the value of the Padé approximant

$$C_N(z) = A_N(z)/B_N(z) \tag{2}$$

at a given point z. The polynomials A_N and B_N are of order $(N-1)/2$ and $(N-1)/2$ for N odd and $(N-2)/2$ and $N/2$ for N even.[1]

When using N-point Padé approximants to calculate Green's functions, one must decide how to choose the input points $i\omega_n$ in order to get a good approximation on the real frequency axis. The temperature obviously determines the distance between adjacent Matsubara points, but even with T fixed, any subset of the point set $\{i\omega_n | n = 1, \ldots\}$ could be used for the Padé algorithm. Since there are very few theoretical results concerning the convergence of the N-point Padé approximant, one is forced to make numerical tests.[2]

For this purpose we applied the Padé scheme to complex functions $F(z)$ analytic in the upper half complex plane and defined, through a spectral representation, by their imaginary parts on the real axis. From the spectral formula we calculated the value of the function at the Matsubara points on the imaginary axis. Using these values as an input for the Padé scheme, we then compared the imaginary part of different Padé approximants with the original spectral function on the real axis.

Because the singularities in the lower half plane determine the shape of the function on the real axis, one gets a measure of the structure of a Padé approximant by counting its number of poles in the lower half plane. For this one can use the Routh–Hurwitz criterion,[3] since the functions to be approximated are either real or pure imaginary on the imaginary axis. We also used standard root-solving procedures to locate the poles and zeros of a Padé approximant from the coefficients of the polynomials $A_N(z)$ and $B_N(z)$ in the formula (2). These results were reliable only for Padé approximants of low order (N smaller than 50).

We show some representative Padé approximants for a very structured test function in Fig. 1, along with the location of their most important poles and zeros. The input points were equally spaced from just above the origin to the point given in the figures. The test results imply that to get a good approximation of a function structured up to some real frequency ω one should use a "sufficient" number of input points taken from the imaginary axis up to several times $i\omega$. Equivalently, one needs imaginary points up to the frequency at which the function on the imaginary axis attains its asymptotic form. The shape of the approximants is in most cases caused by distinct poles and zeros in the lower half plane. The extra poles and zeros not needed to describe the function appear in pairs in the upper half plane or very far away from the origin, and do not affect the behavior on the real axis. The locations shown in the figures were obtained from the root-solving subroutine; direct evaluation of the approximants verifies that the poles and zeros in the upper half plane are very nearly cancelling. A bad approximant is often characterized by a pole–zero pair just above or below the real axis. We emphasize that the test function shown represents a very difficult case; we found excellent agreement for simpler spectral functions.

The occurrence of nearly cancelling poles and zeros in the upper half plane indicates that the number of input points could be reduced without changing the shape of the approximants. However, we found it more time-consuming to find the extra points than to use a Padé approximant of artificially high order. Therefore we always used equally spaced input points for the Padé scheme. The temperature T must be chosen so that there are a sufficient number of Matsubara points in the important region of the imaginary axis. This number depends on how much structure one wants to be able to approximate. We found the following procedure, based on the

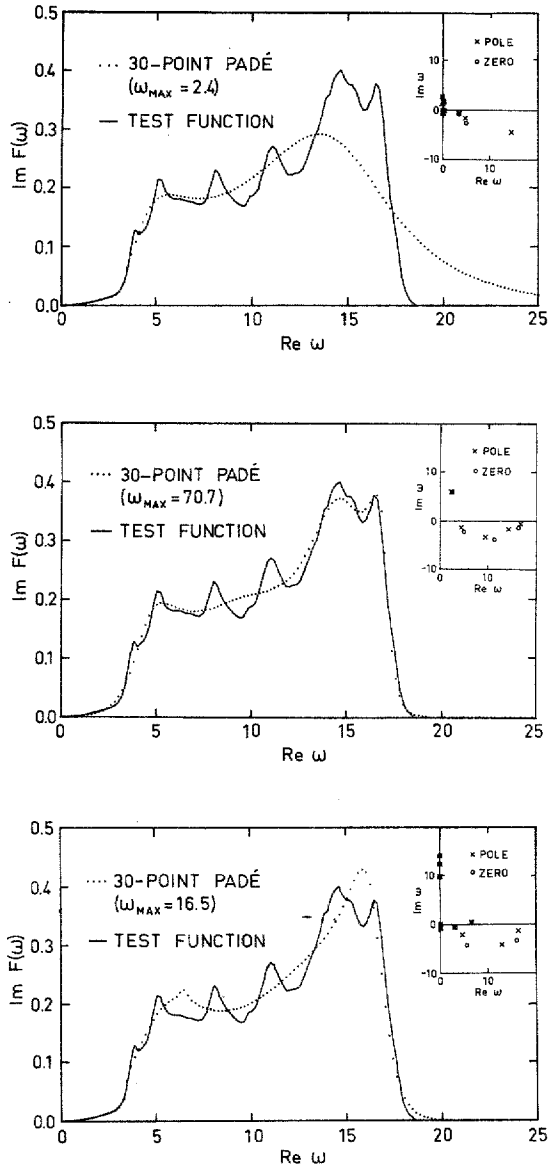

Fig. 1. The imaginary part of different N-point Padé approximants compared with a given test function on the real axis. The input points were equally spaced from $i0.08$ to $i\omega_{max}$. The locations of the most important poles and zeros are shown for the low-order Padé approximants.

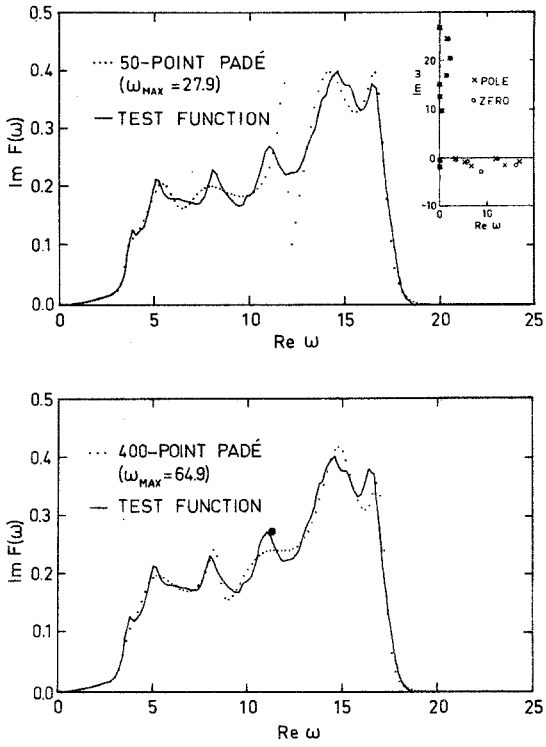

Fig. 1. Continued

Routh–Hurwitz criterion, to be very useful in choosing a good approximant without plotting a great many functions: Given a set of values $\{F(i\omega_n)|n = 1, \ldots, M\}$, we form Padé approximants by calculating the coefficients a_i with the recursion formula (A2), using more and more input points, starting from $i\omega_1$. At regular intervals (e.g., every ten points) we count the number of poles in the lower half plane. This number increases at first, and when it has reached a plateau value a corresponding Padé approximant can be expected to be a good candidate. Approximants corresponding to sudden jumps in the pole number should be avoided. Although this procedure is very rough, we did not succeed in finding any better way of optimizing the choice of input points. The most crucial aspects seem to be the accuracy of the input values $F(i\omega_n)$ and the precision used in the Padé recursions. In our calculations we used double precision (17–18 digits); rounding off the input values to ten digits already meant a significant loss of resolution. Calculating a 200-point Padé approximant at 100 points on the real axis required 7 sec (CPU) on a UNIVAC 1108.

3. APPLICATION: STRONG COUPLING SUPERCONDUCTIVITY

In strong coupling superconductors[4] the retarded part of the effective electron–electron interaction causes strong frequency variations in the self-energy, which can be measured in a tunneling experiment. This frequency dependence is described by the Eliashberg equations for the frequency-dependent gap function Δ and renormalization function Z. The gap function is related to the experimental energy gap Δ_0 and tunneling density of states $N_T(\omega)$ by the formulas

$$\Delta_0 = \mathrm{Re}\Delta(\Delta_0) \tag{3a}$$

$$N_T(\omega) = \mathrm{Re}\frac{\omega}{[\omega^2 - \Delta^2(\omega)]^{1/2}} \qquad (\text{real } \omega) \tag{3b}$$

The solutions of the Eliashberg equations depend on the Coulomb pseudopotential μ^* and the phonon function $\alpha^2(\omega)F(\omega)$, where $F(\omega)$ is the phonon density of states and $\alpha^2(\omega)$ is the electron–phonon coupling. McMillan has developed an inversion program[5] which determines the parameters μ^* and α^2F for which the calculated Δ_0 and $N_T(\omega)$ agree with the experimentally measured quantities. This program solves the Eliashberg equations for the real frequency functions $\Delta(\omega)$ and $Z(\omega)$. The corresponding equations for the imaginary frequency functions $\Delta(i\omega_n)$ and $Z(i\omega_n)$ are much easier to solve, however, and have recently been of great interest, because the thermodynamic properties of superconductors are easily calculated from the solutions $\Delta(i\omega_n)$ and $Z(i\omega_n)$. In the remainder of this paper we discuss the use of N-point Padé approximants to obtain the real frequency functions $\Delta(\omega)$ and $Z(\omega)$ from the calculated functions $\Delta(i\omega_n)$ and $Z(i\omega_n)$.

3.1. Solving the Eliashberg Equations

The imaginary frequency Eliashberg equations for a dirty superconductor are[6]

$$\phi(i\omega_n) = \pi T \sum_m [\lambda(\omega_n - \omega_m) - \mu^*] \frac{\Delta(i\omega_m)}{[\omega_m^2 + \Delta^2(i\omega_m)]^{1/2}} \tag{4a}$$

$$\omega_n Z(i\omega_n) = \omega_n + \pi T \sum_m \lambda(\omega_n - \omega_m) \frac{\omega_m}{[\omega_m^2 + \Delta^2(i\omega_m)]^{1/2}} \tag{4b}$$

where

$$\Delta(i\omega_n) = \phi(i\omega_n)/Z(i\omega_n) \tag{5a}$$

$$\lambda(\omega_n - \omega_m) = \int_0^\infty d\omega\, \alpha^2(\omega)F(\omega) \frac{2\omega}{\omega^2 + (\omega_n - \omega_m)^2} \tag{5b}$$

These equations can be solved straightforwardly by successive iterations. To make the convergence faster, we iterated the ϕ equation 3–5 times per each

Z iteration, because Z is not very sensitive to changes in ϕ. It also appeared that the shape of the ϕ vector converges very fast, whereas its overall magnitude converges more slowly. Therefore we decomposed the ϕ vector by $\phi = \hat{\phi}M$, where $\hat{\phi}(i\omega_1) = 1$, and iterated the magnitude M by solving the equation

$$\sum_n \frac{\hat{\phi}(i\omega_n)\phi(i\omega_n; M)}{\{\hat{\phi}^2(i\omega_n)M^2 + \omega_n^2 Z^2(i\omega_n)\}^{1/2}} \Big/ \sum_n \frac{M\hat{\phi}^2(i\omega_n)}{[\hat{\phi}^2(i\omega_n)M^2 + \omega_n^2 Z^2(i\omega_n)]^{1/2}} = 1$$

with linear interpolation in the two last M points. $\phi(i\omega_n; M)$ is the left-hand side of Eq. (4a) with ϕ replaced by $\hat{\phi}M$ in Eq. (5a).

As input for our calculations we used phonon functions α^2F obtained with McMillan's inversion program and tabulated in Ref. 7. Since the pseudopotential μ^* depends on the actual cutoff $i\omega_c$ used in Eq. (4a), we employed a procedure similar to the M iteration above to progressively adjust μ^* until the energy gap $\Delta_0(\mu^*)$ from a low-order Padé approximant of $\Delta(i\omega_n)$ agreed with the experimental value. We have no reason to believe that the pseudopotential from McMillan's inversion program should be used in an imaginary frequency calculation, even if the cutoff frequencies are the same in magnitude. We discuss this point in more detail in Section 3.2.

We solved the Eliashberg equations (4a) and (4b) for a number of superconductors. One solution required 1–5 min (CPU), depending on the number of Matsubara points (200–500). Figure 2 shows three 199-point

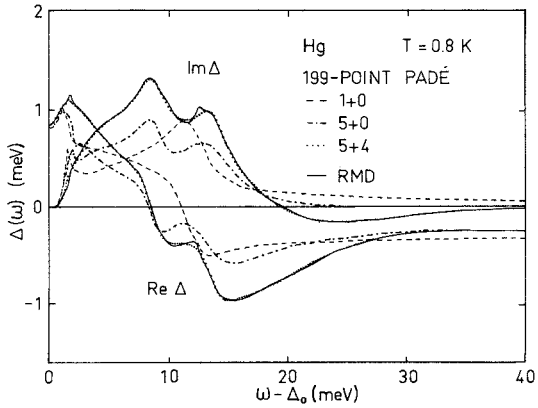

Fig. 2. Three 199-point Padé approximants of the gap function $\Delta(\omega)$ for mercury obtained after 1 iteration (1+0), 5 iterations (5+0) of the linearized Eliashberg and a further 4 iterations (5+4) of the complete equations. The solution of the real frequency equations (RMD) is from Ref. 7.

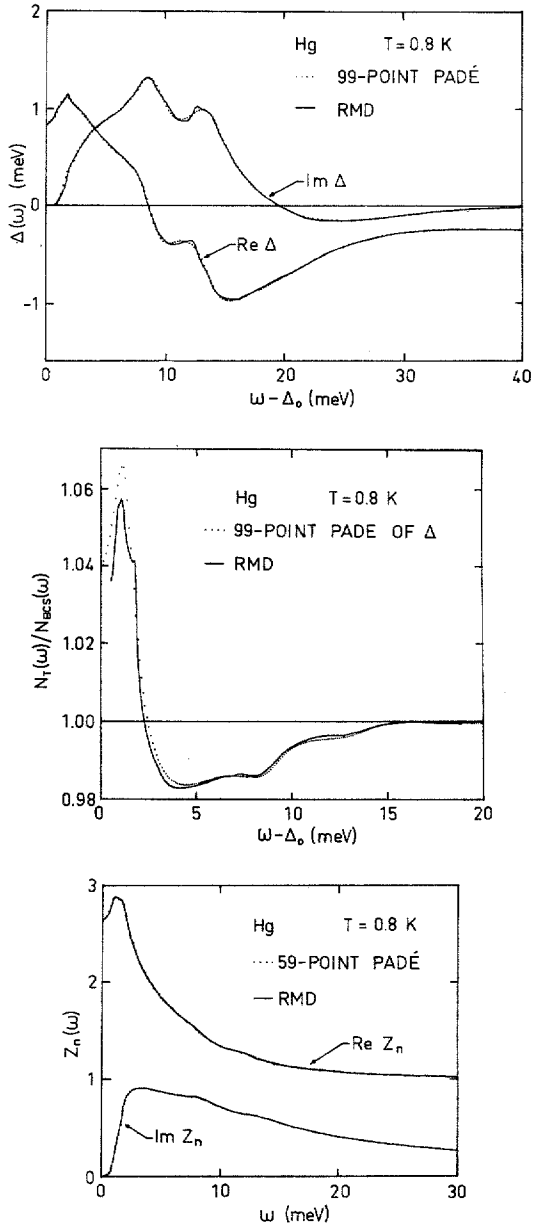

Fig. 3. Padé results for mercury compared with real frequency solutions (RMD) from Ref. 7: the gap function $\Delta(\omega)$, the normalized density of states $N_T(\omega)$, and the normal state renormalization function $Z_n(\omega)$.

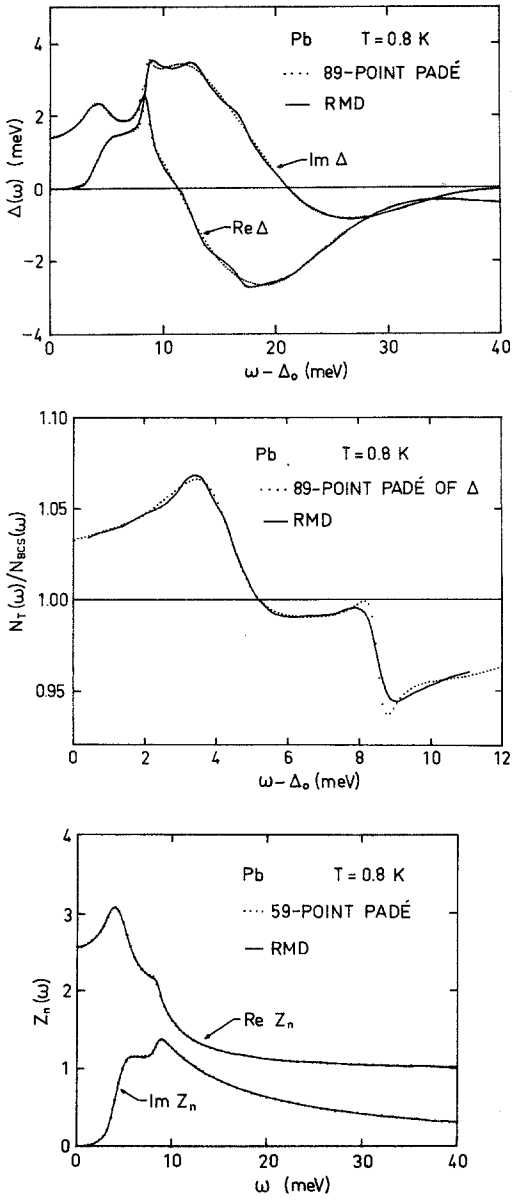

Fig. 4. Padé results for lead compared with real frequency solutions (RMD) from Ref. 7: the gap function $\Delta(\omega)$, the normalized density of states $N_T(\omega)$, and the normal state renormalization function $Z_n(\omega)$.

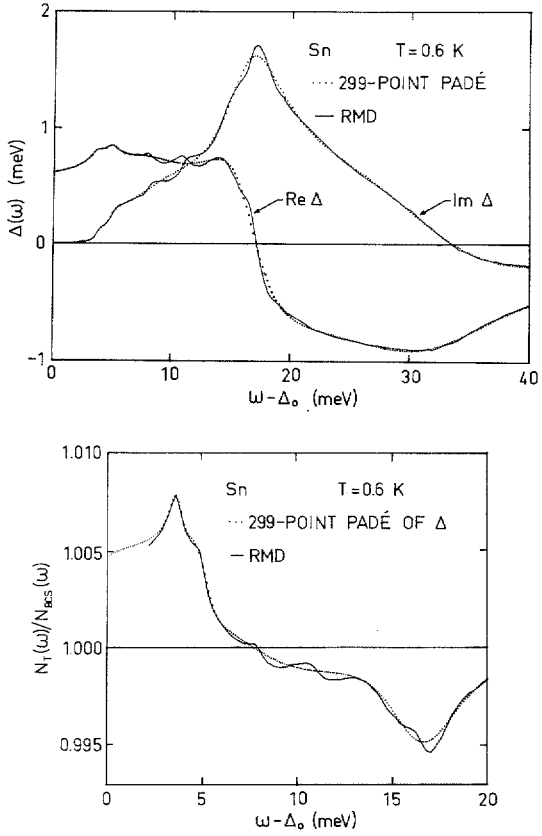

Fig. 5. Padé results for tin compared with real frequency solutions (RMD) from Ref. 7: the gap function $\Delta(\omega)$ and the normalized density of states $N_T(\omega)$.

Padé approximants of the gap function Δ for mercury obtained after different numbers of iterations. Usually we first iterated a linearized version of the gap equation a few times [$\Delta = 0$ in the square roots of Eqs. (4a) and (4b)] and used the resulting ϕ vector as an initial guess for the iterations of the complete equations. The Padé approximant obtained after 5+4 iterations did not improve much with further iterations, as can be seen by comparing with a Padé approximant of the completely converged Δ vector in Fig. 3 (obtained after 50 iterations). We also show the tunneling density of states from formula (3b) normalized against the BCS expression [$\Delta(\omega) \equiv \Delta_0$ in formula (3b)] and the normal state renormalization function Z_n [from Eq. (4b) with $\Delta = 0$], because these functions are tabulated in Ref. 7. The overall

agreement is very good [the tabulated density of states is the experimental one; a direct calculation of $N_T(\omega)$ from the solution $\Delta(\omega)$ agrees better at low frequencies with the curve from the Padé approximant].

A similar comparison of the Padé approximants with the real frequency results for lead is shown in Fig. 4. Here a problem arises with the steep structure at 8 meV. In Fig. 5 we have plotted results for tin, where the phonon-induced variations appear on a finer scale. This fine structure was not resolved in our calculations.

In all cases the agreement with the real frequency results was excellent at small frequencies. This supports the correctness of our iteration procedure, in which we trust the Padé method to give a reliable energy gap $\Delta_0(\mu^*)$ as a function of the pseudopotential μ^*. The approximants shown were chosen with the help of the Routh–Hurwitz criterion, but different approximants did not differ much as long as their pole number remained on the plateau.

We have shown Padé approximants of the gap function and the normal state renormalization function, because these solutions are tabulated in Ref. 7. Similar results were obtained by approximating the pairing self-energy $\phi(\omega)$ and the superconducting renormalization function $Z(\omega)$. The gap function can also be obtained by dividing $\phi(\omega)$ by $Z(\omega)$, but the results do not change significantly from a direct continuation of $\Delta(i\omega_n)$.

3.2. Consistent Choice of μ^* Versus $i\omega_c$

The frequency summation in the gap equation (4a) should extend up to a frequency of the order of the electron bandwidth. In actual calculations the sum is carried out to a much smaller frequency using a pseudopotential to compensate for the neglected terms. If the Eliashberg equations (4a) and (4b) are used to calculate thermodynamic properties of a superconductor with the phonon function $\alpha^2(\omega)F(\omega)$ obtained from McMillan's inversion program, one wants to be sure to use effectively the same pseudopotential as that used in the inversion. As we explained in the previous section, given a fixed cutoff $i\omega_c$ one can employ Padé approximants to find the pseudopotential μ^* that corresponds to the experimental energy gap Δ_0.

We calculated the transition temperature T_c of several superconductors to study the influence of a consistent choice of the pseudopotential vs. cutoff. For the calculations of T_c we used the algorithm given by Bergmann and Rainer.[8] The results are shown in Table I. The experimental energy gap Δ_0, the transition temperature $T_{c,\mathrm{exp}}$, and the temperature T_m at which the tunneling experiment was made are from Ref. 7. McMillan's inversion program used the cutoff ω_c to derive the phonon function α^2F and the pseudopotential μ_1^*. The value μ_2^* was obtained by iterating the Eliashberg equations (4a) and (4b) at the temperature T_m using the cutoff $i\omega_c$ and the

TABLE I

Calculation of the Transition Temperature

Material	Δ_0	$T_{c,\exp}$	T_m	ω_c	μ_1^*	T_{c1}	μ_2^*	T_{c2}
Pb	1.40	7.19	1	60	0.131	7.29	0.1353	7.22
Sn	0.606	3.77	1	120	0.111	3.83	0.1126	3.80
Hg	0.83	4.19	0.35	44	0.11	4.24	0.1139	4.19
Tl	0.366	2.33	0.35	55	0.135	2.28	0.1359	2.27
$Pb_{0.6}Tl_{0.4}$	1.08	6.0	1	60	0.126	5.83	0.1306	5.77
$Pb_{0.6}Bi_{0.2}Tl_{0.2}$	1.50	7.26	1	60	0.137	7.40	0.1396	7.37

given phonon function. The transition temperatures T_{c1} and T_{c2} were calculated with the pseudopotentials μ_1^* and μ_2^*, respectively.

The consistent choice μ_2^* for the pseudopotential in most cases gives a better value for the transition temperature than the real frequency pseudopotential, although the differences are within the limits in which the Eliashberg equations are expected to be accurate. Although the calculated value for μ_2^* depends somewhat on the numerical routine used to evaluate the integral over the pointwise-tabulated phonon function $\alpha^2(\omega)F(\omega)$ in the expression (5b) for $\lambda(\omega_n - \omega_m)$, the value T_{c2} remains very nearly constant as long as the same routine is used in the T_c program.

4. CONCLUDING REMARKS

We have investigated the possibility of using N-point Padé approximants to analytically continue the complex frequency Green's function from the Matsubara points to the real frequency axis. The tests we performed by approximating known functions implied that the resolution obtainable is limited by the number of digits used in calculating the imaginary frequency functions and in the Padé recursions. The results are in any case expected to be worst where the function to be approximated has large variations, because then the approximant will have a pole very near the real axis simulating some perhaps more complicated kind of singularity in the lower half plane.

The Padé method was successfully applied to the solution of the Eliashberg equations. The fine structure of the real frequency functions is, however, not resolved, because, due to the limited numerical precision, the Padé approximants smooth out small variations. Since the temperature determines the difference between the Matsubara points, the Padé method works best at low temperatures, where it offers a way of getting rather accurate solutions of the Eliashberg equations at small computer costs.

APPENDIX

There exists a fast algorithm for calculating an N-point Padé approximant to a function, given its values u_i at N complex points z_i $(i = 1, \ldots, N)$[1]: We define the continued fraction

$$C_N(z) = \frac{a_1}{1+} \frac{a_2(z-z_1)}{1+} \cdots \frac{a_N(z-z_{N-1})}{1} \tag{A1}$$

where the coefficients a_i are to be determined so that

$$C_N(z_i) = u_i, \qquad i = 1, \ldots, N$$

The coefficients a_i are then given by the recursion

$$\begin{aligned} &a_i = g_i(z_i), \qquad g_1(z_i) = u_i, \qquad i = 1, \ldots, N \\ &g_p(z) = \frac{g_{p-1}(z_{p-1}) - g_{p-1}(z)}{(z-z_{p-1})g_{p-1}(z)}, \qquad p \geqq 2 \end{aligned} \tag{A2}$$

The recursion formula for continued fractions finally yields

$$C_N(z) = A_N(z)/B_N(z)$$

where

$$\begin{aligned} A_{n+1}(z) &= A_n(z) + (z-z_n)a_{n+1}A_{n-1}(z) \\ B_{n+1}(z) &= B_n(z) + (z-z_n)a_{n+1}B_{n-1}(z) \end{aligned} \tag{A3}$$

and

$$A_0 = 0, \qquad A_1 = a_1, \qquad B_0 = B_1 = 1$$

The algorithm is most efficiently used to directly calculate the value of the approximant at a given point by means of the recursion formula (A3), although it also can give the coefficients of the polynomials $A_N(z)$ and $B_N(z)$.

ACKNOWLEDGMENTS

The authors thank Dierk Rainer for numerous useful suggestions, and John Wilkins for a remark which stimulated this investigation.

REFERENCES

1. G. A. Baker Jr., *Essentials of Padé Approximants* (Academic Press, New York, 1975), Chapter 8.
2. R. W. Haymaker and L. Schlessinger, in *The Padé Approximant in Theoretical Physics*, G. A. Baker, Jr. and J. L. Gammel, eds. (Academic Press, New York, 1970), Chapter 11.
3. R. C. Dorf, *Modern Control System* (Addison-Wesley, London, 1970), p. 113.
4. D. J. Scalapino, in *Superconductivity*, R. D. Parks, ed. (Marcel Dekker, New York, 1969), Chapter 10.
5. W. L. McMillan and J. M. Rowell, in *Superconductivity*, R. D. Parks, ed. (Marcel Dekker, New York, 1969), Chapter 11.
6. D. Rainer and G. Bergmann, *J. Low. Temp. Phys.* **14**, 501 (1974).
7. J. M. Rowell, W. L. McMillan, and R. C. Dynes, *J. Phys. Chem. Ref. Data*, to be published.
8. G. Bergmann and D. Rainer, *Z. Physik* **263**, 59 (1973).